Acoustic phonon propagation and elastic properties of nano-sized carbon films investigated by Brillouin light scattering

M.G. Beghi[a,*], C.S. Casari[a], A. Li Bassi[a], C.E. Bottani[a], A.C. Ferrari[b], J. Robertson[b], P. Milani[c]

[a]INFM and Nuclear Engineering Dept., Politecnico di Milano, Via Ponzio 34/3, 20133 Milan, Italy
[b]Engineering Department, Cambridge University, Trumpington Road, Cambridge CB2 1PZ, UK
[c]INFM and Physics Department, Università di Milano, Via Celoria 16, 20133 Milan, Italy

Abstract

Carbon films having a structure at the nanometer scale are of paramount interest. Experimental tools for the mechanical characterization of such materials are still an open issue, due to the relevance of mesoscopic scales. Brillouin light scattering by acoustic phonons of sub-micrometric wavelength is among the few techniques sensitive at the appropriate length scale. Elastic properties can be derived from measured acoustic properties, if the film thickness and mass density are independently measured, typically by X-ray reflectivity. Applications to two very different types of films are discussed. Tetrahedral amorphous carbon (ta-C) films of high density and stiffness can be deposited with thickness down to a few nanometers. We show that combining Brillouin scattering and X-ray reflectivity the elastic properties of films can be measured for thicknesses down to 2 nm. We also measure the dependence of stiffness on thickness, finding that the high stiffness of thicker ta-C films is reached for thicknesses of approximately 10 nm. Films deposited by low energy cluster beam deposition are characterized by granularity and porosity at scale lengths ranging from nanometers to micrometers. We show that Brillouin scattering discriminates well among films compact enough to support the propagation of acoustic phonons and films in which such phonons are confined and/or over-damped. When acoustic propagation is supported the elastic properties can be obtained, at wavelengths of hundreds of nanometers. It is thus shown that Brillouin scattering has a peculiar potential for the characterization of films having structures of nanometric size.
© 2002 Elsevier Science B.V. All rights reserved.

Keywords: Elastic properties; Light scattering; Carbon; Coatings

1. Introduction

Nanostructured carbon materials of various types are of paramount interest both for pure and applied science [1]. Various relevant properties of such materials, including the mechanical ones, are determined by their structure at a mesoscopic rather than atomic or molecular level. Consequently, their characterization is still an open question because a few experimental probes are sensitive at the appropriate length scale. For mechanical characterization, techniques such as indentation and laser induced ultrasonics become critical. In this work we show that surface Brillouin scattering (SBS) of visible light, i.e. scattering of light by surface acoustic waves (SAWs) [2–4], is able to characterize the elastic properties of such materials at scales ranging from nanometers to micrometers. SBS is intrinsically contact-less and non-destructive; it probes acoustic phonons at sub-micrometer wavelengths, and supplies the acoustic characterization at this length scale. Relevant information on the material structure at a mesoscopic level is thus gained.

Two types of carbon materials of markedly different properties are analyzed here: tetrahedral amorphous carbon (ta-C) films of nanometric thickness, deposited by a filtered cathodic vacuum arc (FCVA) [5,6], and films produced by low energy cluster beam deposition (LECBD) [7–9] under various conditions. Ta-C is a high density and stiffness material, deposited 'atom by atom' by carbon ions. At length scales sufficiently larger than the interatomic distance its mechanical behavior is conveniently modeled by standard continuum mechanics. In contrast, materials deposited by LECBD have low density and are three-dimensionally nanostructured: during deposition cluster fragmentation is almost negligible, the aggregates maintain their individuality and assemble themselves in structures hierarchically organ-

*Corresponding author. Tel.: +39-02-2399-6351; fax: +39-02-2399-6309.

E-mail address: marco.beghi@polimi.it (M.G. Beghi).

ized over length scales from tens of nanometers up to microns [10], giving a material which is granular at a nanometer scale. The resulting structure has interesting properties for field emission and electrochemical applications. For this kind of material the continuum mechanical model might not be fully appropriate, since mesoscopic length scales can be relevant.

For both types of materials elastic characterization at scales ranging from nanometers to hundreds of nanometers provides significant information. In films having thicknesses of tens of nanometers ta-C has a high stiffness, comparable with that of crystalline diamond [11]; there is, however, evidence of interface and surface layers of lower density and lower stiffness [5]. It is interesting to ascertain whether the peculiar stiffness of ta-C is preserved when the thickness is reduced to a few nanometers. This is relevant, since carbon coatings of thickness down to 2 nm are needed to further increase the storage density in magnetic hard disks and reach the 100 Gbit inch^{-2} target [12]. LECBD materials can have different properties at mesoscopic scales, depending on the deposition conditions, namely the initial cluster mass distribution. They resemble other types of low-density carbon materials, such as porous carbon and carbon aerogels [1]. The characterization of their elastic properties is particularly interesting because it offers the possibility of studying the evolution, towards a continuous homogeneous medium, of a system characterized by granularity and porosity at different length scales.

The elastic properties are derived from the characterization of the acoustic behavior, if the film thickness (when thickness is not larger than acoustic wavelength) and mass density are known. These quantities can be measured by X-ray reflectivity (XRR) [5,13]. SBS can overcome the problems typical of nano-indentation when dealing with very thin films or granular and soft materials [14].

SBS is typically applied to homogeneous compact films with perfect surfaces and buried interfaces. In particular, SBS has been extensively exploited to characterize the elastic properties of various compact films, including hydrogenated amorphous carbon films [16–18], thick (hundreds of microns) CVD diamond films [19,20], ta-C films grown by FCVA techniques [11,21], and sub-millimetric particles of hard material synthesized from fullerenes [22]. All these measurements refer to film thicknesses above 100 nm, up to hundreds of micrometers. Only a very few measurements have been reported in the thickness range of tens of micrometers [11,17]. In this work the technique is pushed to thicknesses of a few nanometers.

Fewer references are available for LECBD films. It was shown that SBS can be used to characterize such carbon films of thickness of approximately 100 nm [14]; however, the roughness and inhomogeneity of LECBD systems can, a priori, pose serious problems to a system-

atic use of SBS and, in general, to a precise determination of the elastic constants and of their dependence on the mesoscopic organization of the precursor clusters. A systematic analysis is presented in this work.

2. Experimental

2.1. Specimen preparation

2.1.1. ta-C films
ta-C films were deposited at floating potential using a FCVA source with an integrated off plane double bend (S-bend) magnetic filter. The beam was defocused to have a slow growth and a better control of very small thicknesses, down to a few nanometers. Sets of films were grown for increasing deposition times on the (001) face of silicon substrates [5]. A set of samples was analyzed, which includes a bare silicon substrate and ta-C films of different thickness. The 'bare' substrate is in reality covered by a nanometric layer of native oxide, due to exposure to air. Although this layer was removed before ta-C deposition, some contamination cannot be completely ruled out.

2.1.2. Cluster assembled films
Nanostructured carbon films were deposited from a supersonic cluster beam produced by a pulsed microplasma cluster source [23]. In standard operation conditions the clusters in the beam have sizes below 1500 atoms, with a log-normal distribution peaked at approximately 500 atoms/cluster. The kinetic energy of the clusters was of the order of 0.2 eV per atom, meaning that no substantial cluster fragmentation is expected [8]. Exploiting aerodynamic focusing effects it was possible to control and select the cluster mass distribution and deposition rates [24], in particular selecting a focused beam containing only the smaller clusters (below 500 atoms). Films were deposited on both silicon and a smooth highly reflecting aluminum substrate. Aluminum substrate gave better results in SBS measurements, because silicon has a lower reflectivity and also has an intense central peak, due to a two-phonon Raman scattering, which overlaps the surface peaks of interest.

With the standard cluster mass distribution the deposition rate was 4–5 nm min^{-1} and the density of the films, measured by XRR (see below), turned out to be 0.8–0.9 g cm^{-3}. With the focused beam, containing only the smaller clusters, the source was adjusted for a deposition rate of 5 nm s^{-1}, and the density of the films turned out to be 1.2–1.3 g cm^{-3}. In both conditions we deposited films with thicknesses ranging from 30 nm to more than 1 μm. The primeval clusters coalesce into larger units: the small cluster film is characterized by grains with a typical diameter of 20–30 nm, whereas the large cluster film has grains with a diameter of several hundreds of nanometers. Cluster size strongly

affects the evolution of film roughening: in the films deposited with small clusters the roughness is a factor of three lower than that of the film assembled with large clusters.

2.2. Measurements

2.2.1. X-Ray reflectivity

The thickness and density of the films were derived by specular XRR measurements made on a Bede GXR1 reflectometer using CuK_β radiation. The data were fitted to the scatter simulated from model structures using the Bede REFS-MERCURY code [5,25,26]. Measurements performed on these same ultra-thin ta-C films were already discussed in detail [26,27], showing that this technique is able to reliably characterize films of thickness down to 2 nm. The density cannot simply derived from the critical angle (as it is done for thicker films), but must obtained from the fit of the whole reflectivity curve to a model structure [26,27].

2.2.2. Surface Brillouin scattering

SBS measurements were performed in backscattering with an Argon ion laser operating at $\lambda_0 = 514.5$ nm. The scattered light was collected without polarization analysis; its spectrum was measured by a tandem $3+3$ pass high contrast interferometer of the Sandercock type [2] with a finesse of approximately 100. LECBD samples were kept in vacuum to prevent damage by photo-oxidation effects [28]. The aluminum substrates were isotropic; for films grown on the (001) face of Si substrates SAW propagation was along the [100] direction.

SAWs have a wavevector $q_{||}$ parallel to the surface, and a velocity v_{SAW} which can depend on wavelength. SAW dispersion relations $v_{SAW}(q_{||})$ are obtained by a set of measurements at different incident angles θ_i, since, in backscattering, $q_{||} = (4\pi/\lambda_0) \sin \theta_i$.

SBS relies on thermally excited acoustic waves, whose amplitude is much smaller than that of the excited waves probed by other acoustic techniques. Measurements are therefore time consuming: acquisition times up to several hours can be required. However, the measurement is intrinsically contact-less and local (measurement is over the focusing spot of the laser, i.e. tens of microns). The probed acoustic wavelengths can be significantly smaller than those probed by any other technique, giving Brillouin scattering a peculiar potential in terms of spatial resolution, particularly relevant in the case of thin films, and of sensitivity to mesoscopic scales.

3. Results and data analysis

3.1. Derivation of the elastic properties

The Rayleigh wave (RW) at the surface of a bare substrate, the prototype of SAWs, has a velocity inde-

pendent from wavelength, and a displacement field which decays exponentially with depth, the decay length being the same as the wavelength $\lambda_{||} = 2\pi/q_{||}$ [2]. When a surface layer of thickness h is present, it modifies the spectrum of the substrate SAWs. The RW becomes the modified Rayleigh wave (MRW), whose velocity is a function of $q_{||}h$ [4]. In very thin films ($q_{||}h \ll 1$) the MRW displacement field is mostly in the substrate. However, close to the surface, where the wave amplitude and energy density are maximum, the MRW propagates in the film and senses its properties. At higher values of $q_{||}h$ the MRW is more confined in the film and more sensitive to its properties. Therefore for films acoustically faster/slower than the substrate the MRW velocity is an increasing/decreasing function of $q_{||}h$.

Acoustically slow films can act as wave-guides, and support surface acoustic modes mainly confined in the film itself (Sezawa waves) [2–4]. Pseudo surface acoustic mode also exist: they are not strictly SAWs, but their displacement field is mostly in the vicinity of the surface. An important pseudo surface wave is longitudinally polarized, and is called longitudinal resonance (LR) [2–4].

The velocities of SAWs in layered structures can be computed by the continuum elastodynamics equations as a function of the density and the elastic constants of the film and the substrate, and of h and $q_{||}$ [4,15]. The elastic constants can then be obtained fitting the computed velocities to the measured ones [11,13,15]. Films which are isotropic at the wavelength scale (hundreds of nanometers for SBS) have elastic constants completely determined by only two moduli such as the Young's modulus E and shear modulus G. The data analysis gives a confidence region in the (E,G) plane and can be supplemented by physical plausibility criteria[15]. The (E,G) couple is adopted because a detailed sensitivity analysis [29] showed that these two moduli are better determined; the uncertainties on Poisson's ratio ν or bulk modulus B remain much higher.

3.2. Tetrahedral amorphous carbon films

The film thickness and mass density, measured by XRR, are presented in Table 1. Some indication of film layering can be found, and the mean density (~ 2.8 g cm^{-3}), smaller than that of thick films (~ 3.3 g cm^{-3}), shows that the surface and interface layers have the effect of reducing the mean density. In the analysis of acoustical data films are, however, modeled as a single homogeneous equivalent layer.

SAW dispersion relations for the various films, measured by SBS, are shown in Fig. 1. Data were analyzed adopting accepted values for properties of silicon ($\rho = 2.33$ g cm^{-3}, $C_{11} = 166$ GPa, $C_{12} = 63.9$ GPa, $C_{44} = 79.6$ GPa). The 90%-confidence regions in the (E,G) plane

Table 1
Thickness h and mass density ρ of ta-C films, derived from XRR measurements

Sample	h (nm)	ρ (g/cm³)	E (GPa)	G (GPa)
1	2.2	2.8	95 ± 30	40 ± 20
2	3.5	2.8	195 ± 30	85 ± 30
3	4.5	2.8	220 ± 40	100 ± 30
4	8	2.8	380 ± 40	170 ± 45
[11]	76	3.3	750 ± 40	340 ± 50

Young's modulus E and shear modulus G obtained as 90% confidence intervals from the SBS data fit. For comparison: data from Ferrari et al. [11].

are found [27]. Only the part of the confidence regions satisfying physical plausibility criteria is considered: it is assumed that the carbon films have a positive Poisson's ratio ν and a bulk modulus $B < B_{diamond} = 445$ GPa. The resulting intervals of the (E,G) couple are reported in Table 1. The lines in Fig. 1 are computed from the most probable values.

The dispersion relations of Fig. 1 identify a well-defined trend. The sequence starting from the oxide film and continuing with the ta-C films in order of increasing thickness corresponds to a marked increase of film stiffness. The dispersion relation $v_{MRW}(q_{||}h)$ of the oxide film is decreasing, indicating that the oxide is acoustically slower than silicon. The dispersion relation for the 2.2 nm, 3.5 nm, 4.5 nm and 8 nm ta-C film progressively shifts from moderately decreasing (2.2 nm) to increasing (3.5 nm and 4.5 nm, which are similar) and steeply increasing (8 nm). This indicates that the 2.2 nm film is still acoustically slower than the Si substrate, but stiffer than the native oxide, that the 3.5 nm and 4.5 nm films are stiffer than Si, and that the 8 nm film is markedly stiffer than Si. The resulting values of the moduli, reported in Table 1, show that for the 8 nm film the elastic moduli begin to be comparable with those found for thicker ta-C films [11].

With these ultra-thin films both SBS and XRR are pushed to their sensitivity limits; in particular SBS measurement relies on the perturbation of an acoustic wave by a layer of the order of one-hundredth of the wavelength. The robustness of the results for the film elastic constants was therefore checked [27]. It was found that, due to the very small film thickness, the most critical input is the stiffness of the substrate. The availability of measurements on different films allowed us to conclude that the above values of silicon elastic constants are at most overestimated by a fraction of a percent, and that consequently the film elastic constants of Table 1 could be underestimated, by a few percent at most.

3.3. Cluster assembled carbon films

XRR measurements gave the values of film thickness and mass density mentioned above. SBS spectra meas-
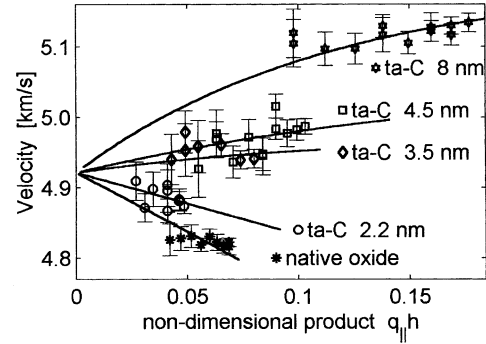

Fig. 1. Measured and computed dispersion relations (acoustic velocity vs. non-dimensional product $q_{||}h$) for oxide-covered silicon substrate and ta-C films of increasing thickness (see Table 1).

ured from films grown from large clusters are discussed first. In thin films grown on aluminum substrates, despite the relatively high surface roughness, which increases with film thickness, surface peaks due to interactions with Rayleigh and (not always) Sezawa waves can be detected up to a critical thickness of the order of 200 nm. The frequencies and intensities of the peaks vary with film thickness (see Fig. 2). When the thickness increases above roughly 100 nm a central peak starts to develop, and the surface peaks become broader. Above approximately 200 nm the surface peaks disappear (see Fig. 2). In the thickest films (above 1 μm) only the central peak and, sometimes, strongly damped bulk acoustic phonons, with a typical wavelength $\lambda_{ph} \sim 200$ nm, have been detected. The bulk feature is due to scattering from a longitudinal phonon, and indicates that at a length scale above λ_{ph} some films can still support acoustic waves. This means that they roughly behave as a continuum with approximate translational invariance and effective elastic constants, although structural dis-
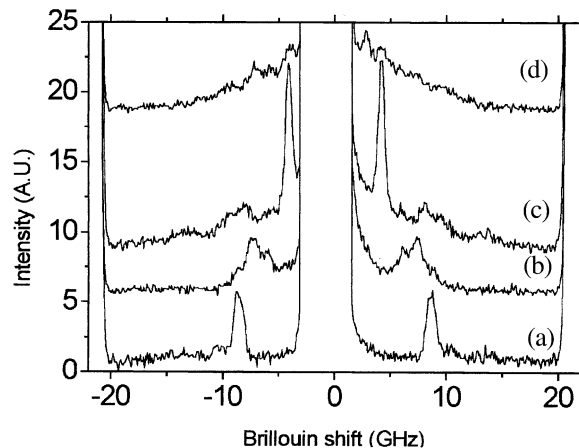

Fig. 2. Brillouin spectra from films, deposited using unfocused beams (larger clusters), of different thickness (A = 30 nm, B = 100 nm, C = 170 nm, D = 350 nm). All the measurements in backscattering, with incidence angle $\theta_i = 50°$.
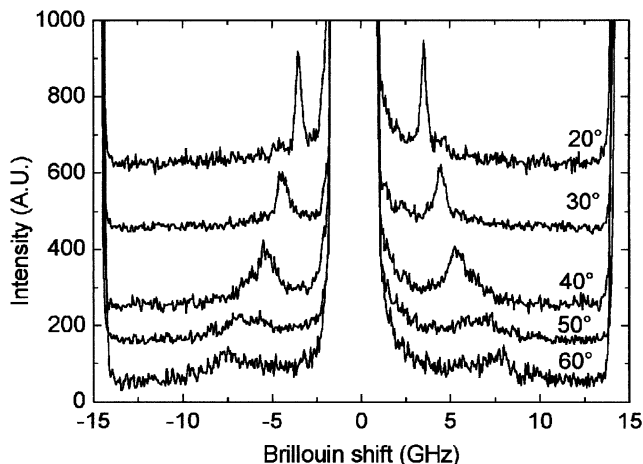
Fig. 3. Brillouin spectra from a thin (∼100 nm) film deposited by an unfocused cluster beam. Measurements in backscattering at various incidence angles θ_i. The peak is due to the modified Rayleigh wave; its frequency scales as $\sin(\theta_i)$. The weak, broad feature centered at null frequency is also visible.

order at smaller scales scatters the phonons significantly. The rather strong central peak in the spectra could be due to non-propagating (overdamped), or confined vibrational excitations, probably connected with different characteristic correlation lengths less than λ_{ph}, related mainly to the huge surface roughness.

In the thinner films, the detection of the Rayleigh and Sezawa waves allows to measure their dispersion relation (see Fig. 3) and to determine the elastic moduli E and G. E varies in the range 3–7 GPa, while G lies in the range 1–2.5 GPa, depending on several cluster source operating parameters, i.e. on the specific properties of the beam and on the exact cluster mass distribution. Very low values of the Poisson's ratio ν (∼0.1) were also estimated. Since the uncertainty in the determination of ν is large, the actual value of ν could be very close to zero, or even negative.

The SBS spectra measured from films grown from smaller clusters are dominated by a sharp MRW peak [30], not expected in low-density granular materials [8]. This indicates that long life acoustic phonons can propagate in the film, meaning that at mesoscopic scale the film appears as a homogeneous elastic continuum; the relatively low surface roughness introduces a small acoustic damping but does not hinder phonon propagation. This behavior is consistent with the picture of a smooth film of a relatively compact material, made of small clusters. In these films the roughness increases very slowly with thickness.

Fig. 4 shows the sharp MRW peaks, and the absence of a central peak evolution. Thus, in this case, the study of thick films is possible, and is advantageous because a thick film behaves as a semi-infinite medium: the acoustic waves propagating in it are not affected by the

presence of the substrate and by the thickness value. Fig. 4 shows that, beside the MRW peak, two other peaks are detected. The first one is identified as the longitudinal resonance (LR, see above) because its frequency scales as $\sin(\theta_i)$. The second one, whose frequency is independent from θ_i, is due to a bulk longitudinal wave. The velocities of these waves allow the derivation of the elastic constants, which are, typically, $C_{11} = 5.4$ GPa and $C_{44} = G = 2.5$ GPa. From these values the mean values $E = 5.3$ GPa, $B = 2.1$ GPa and $\nu = 0.07$ can be estimated. Since the error band in the determination of ν is wide, the possibility of values close to or less than zero cannot be excluded.

4. Conclusions

It was shown that Brillouin scattering has a significant potential for the characterization of carbon films at scales ranging from nanometers to hundreds of nanometers. Brillouin scattering is intrinsically contact-less, non-destructive and local. Acoustic characterization at sub-micrometer wavelength is sensitive enough to detect the perturbation due to nanometer thick layers. Exploited in conjunction with X-ray reflectivity, it allowed the measurement of the elastic constants of nanometer thick ta-C films. Density of approximately 2.8 g cm^{-3} and non-negligible stiffness are measured for thickness down to 2–3 nm. The elastic constants of such ultra-thin layers increase steeply with thickness, and become comparable with those of thicker films at a thickness of the order of 10 nm.

Films grown by low energy cluster beam deposition are characterized by granularity and porosity at scale lengths ranging from nanometers to micrometers. Brillouin scattering supplies significant information at these scales, since it discriminates among inhomogeneities at
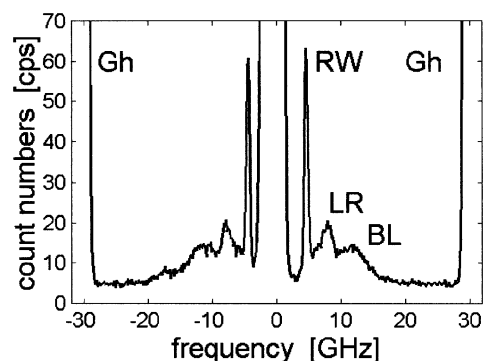

Fig. 4. Brillouin spectrum from a thick film grown with a focused cluster beam, measured in backscattering at incidence angle $\theta_i = 60°$. The peaks correspond to the film Rayleigh wave (RW), the longitudinal resonance (LR) and a bulk longitudinal wave (BL). The strong peak at null frequency shift is due to the elastically scattered laser light, while the two peaks (Gh) are instrumental ghosts, typical of a Fabry–Perot interferometer.

the nanometer or tens of nanometers scale, and those at larger scale. Inhomogeneities at the nanometric scale do not prevent propagation of acoustic waves of hundreds of nanometers wavelength, which are instead damped or scattered by inhomogeneities at a scale similar to their same wavelength. When wave propagation is still supported, the elastic constants are measured at the hundreds of nanometers scale. Such elastic constants are determined by the inter-cluster rather than the intra-cluster interaction, and thus give information on cluster aggregation. Brillouin scattering is therefore a method of choice for the characterization of cluster assembled films.

Acknowledgments

References

[1] M.S. Dresselhaus, G. Dresselhaus, P.C. Eklund, Science and Technology of Fullerenes and Carbon Nanotubes, Academic Press, New York, 1996, p. 281.

[2] F. Nizzoli, J.R. Sandercock, in: G. Horton, A. Maradudin (Eds.), Dynamical Properties of Solids, North-Holland, Amsterdam, 1990.

[3] P. Mutti, C.E. Bottani, G. Ghislotti, M.G. Beghi, G.A.D. Briggs, J.R. Sandercock, in: A. Briggs (Ed.), Advances in Acoustic Microscopy, 1, Plenum Press, New York, 1995, p. 249.

[4] J.D. Comins, in: M. Levy, et al. (Eds.), Handbook of Elastic Properties of Solids, Liquids and Gases, 1, Academic Press/ Harcourt Publishers Ltd, Sidcup, UK, 2000, p. 349.

[5] A.C. Ferrari, A. Li Bassi, B.K. Tanner, V. Stolojan, J. Yuan, L.M. Brown, S.E. Rodil, B. Kleinsorge, J. Robertson, Phys. Rev. B 62 (2000) 11089.

[6] K.B.K. Teo, S.E. Rodil, J.T.H. Tsai, A.C. Ferrari, J. Robertson, W.I. Milne, J. Appl. Phys. 89 (2001) 3706.

[7] D. Donadio, L. Colombo, P. Milani, G. Benedek, Phys. Rev. Lett. 83 (1999) 776.

[8] P. Milani, S. Iannotta, Cluster Beam Synthesis of Nanostructured Materials, Springer, Berlin, 1999.

[9] E. Barborini, P. Piseri, A. Podestà, P. Milani, Appl. Phys. Lett. 77 (2000) 1059.

[10] P. Milani, P. Piseri, E. Barborini, A. Podestà, C. Lenardi, J. Vac. Sci. Technol. A 19 (2001) 2025.

[11] A.C. Ferrari, J. Robertson, M.G. Beghi, C.E. Bottani, R. Ferulano, R. Pastorelli, Appl. Phys. Lett. 75 (1999) 1893.

[12] J. Robertson, Thin Solid Films 383 (2001) 81.

[13] M.G. Beghi, C.E. Bottani, P.M. Ossi, T. Lafford, B.K. Tanner, J. Appl. Phys. 81 (1997) 672.

[14] C.E. Bottani, A.C. Ferrari, A. Li Bassi, P. Milani, P. Piseri, Europhys. Lett. 42 (1998) 431.

[15] M.G. Beghi, C.E. Bottani, R. Pastorelli, in: C. Muhlstein, S.B. Brown (Eds.), Mechanical Properties of Structural Films, ASTM STP 1413, American Society for Testing and Materials, West Conshohocken, PA, 2001.

[16] X. Jiang, J.W. Zou, K. Reichelt, P. Grunberg, J. Appl. Phys. 66 (1989) 4729.

[17] T. Wittkowski, V. Wiehn, J. Jorzick, K. Jung, B. Hillebrands, Thin Solid Films 368 (2000) 216.

[18] L. Valentini, J.M. Kenny, G. Carlotti, G. Socino, L. Lozzi, S. Santucci, J. Appl. Phys. 89 (2001) 1003.

[19] X. Jiang, J.V. Harzer, B. Hillebrands, Ch. Wild, P. Koidl, Appl. Phys. Lett. 59 (1991) 10551.

[20] J.K. Krüger, J.P. Embs, S. Lukas, U. Hartmann, C.J. Brierley, C.M. Beck, R. Jimenez, P. Alnot, O. Durand, J. Appl. Phys. 87 (2000) 74.

[21] M. Chirita, R. Sooryakumar, H. Xia, O.R. Monteiro, I.G. Brown, Phys. Rev. B 60 (1999) R5153.

[22] P.V. Zinin, M.H. Manghnani, S. Tkachev, X. Zhang, A.G. Lyapin, V.H. Brazhkin, I.A. Trojan, Mater. Res. Soc. Symp. Proc. 675 (2001) W11.9.1.

[23] E. Barborini, P. Piseri, P. Milani, J. Phys. D: Appl. Phys. 52 (1999) L105.

[24] P. Piseri, A. Podestà, E. Barborini, P. Milani, Rev. Sci. Instrum. 27 (2001) 2261.

[25] M. Wormington, I. Pape, T.P.A. Hase, B.K. Tanner, D.K. Bowen, Phil. Mag. Lett. 74 (1996) 211.

[26] B.K. Tanner, A. Libassi, A.C. Ferrari, J. Robertson, Mater. Res. Soc. Symp. Proc. 675 (2002) W11.4.

[27] M.G. Beghi, A.C. Ferrari, C.E. Bottani, A. Libassi, B.K. Tanner, K.B.K. Teo, J. Robertson, Diamond Relat. Mater. 11 (2002) 1062.

[28] P. Milani, C.E. Bottani, A. Parisini, G.P. Banfi, Appl. Phys. Lett. 72 (1998) 293.

[29] R. Pastorelli, S. Tarantola, M.G. Beghi, C.E. Bottani, A. Saltelli, Surf. Sci. 468 (2000) 37.

[30] C. Casari, A. Li Bassi, C.E. Bottani, E. Barborini, P. Piseri, A. Podestà, P. Milani, Phys. Rev. B 64 (2001) 085417.